scientific reports

Check for updates

OPEN

Ex vivo evaluation of anti-migration forces of ureteral self-expanding metal stents with different flange designs

Jiaywei Tsauo, Zhiqiang Mo, Qi Wang, Qing Gou, Qicong Mai, Zide Chen & Jing Zhang✉

To evaluate the anti-migration forces of ureteral self-expanding metal stents (SEMS) with various flange designs. In the initial study, 240 fresh porcine ureters were divided into ten groups to evaluate ten custom-made SEMS (Type I–X). Type I and II lacked flanges (8 mm and 10 mm diameters, respectively), while Types III–X had various proximal flange designs. In the subsequent study, 96 ureters were divided into four groups to evaluate four SEMS: a custom-made prototype with the same flange design as Type X (double-stepped shoulders) and three commercial stents, including Urexel, Uventa, and Allium. Proximal and distal anti-migration forces were measured using a universal testing machine. In the initial study, only Type X demonstrated a significantly higher distal anti-migration force than the 8-mm non-flanged SEMS (Type I) ($P = 0.001$). None of the SEMS (Types II–X) showed significantly higher proximal anti-migration force compared to Type I (all > 0.05). In the subsequent study, Uventa demonstrated significantly higher proximal and distal anti-migration forces than the prototype ($P < 0.001$ and $P = 0.001$, respectively). The prototype demonstrated significantly higher proximal and distal anti-migration forces than Urexel (both $P < 0.001$). Allium unraveled during initial testing and was excluded from the analysis. Only the double-stepped shoulders improved distal anti-migration force among eight flange designs. Compared with commercial SEMS, the prototype featuring this design demonstrated higher anti-migration force than Urexel but lower than Uventa.

Keywords Urinary tract, Ureter, Stents, self expandable metallic stents, Prosthesis design

Self-expanding metal stents (SEMS) are increasingly used to treat malignant and benign ureteral strictures[1–3]. Compared with polymeric double-J stents (DJS), SEMS are less prone to encrustations due to their larger caliber, thereby reducing the need for frequent stent exchanges[4]. Furthermore, SEMS provide superior crush resistance, leading to improved stent patency for extrinsic ureteral strictures[4–6]. Moreover, SEMS minimize irritation symptoms by stenting only the stricture, unlike DJS, which span the entire ureter and extend into the bladder. However, a major drawback of SEMS is their high rate of stent migration (as high as 81%)[7–11]. This is primarily attributed to the covering membrane, which prevents tissue and tumor ingrowth and thereby maintains stent patency and enables stent removal, but reduces anti-migration force[12]. In contrast, uncovered SEMS are known for their low rate of stent migration (as low as 0%), but are associated with a high rate of tissue and tumor ingrowth (as high as 64%) and are virtually impossible to remove[13,14].

The stent migration rate for newer covered SEMS (as high as 24%) is reported to be considerably lower than that of older covered SEMS (as high as 81%), likely due to the incorporation of anti-migration features (e.g., flares and double-layer designs)[7–11]. However, stent migration still occurs in a notable proportion of patients and often shortly after SEMS placement, resulting in early re-obstruction and necessitating re-intervention for stent removal and re-stenting[9–11]. Stent migration also remains a well-recognized issue for esophageal SEMS[15]. To mitigate this, flanges have been incorporated at both ends of esophageal stents, a feature now considered standard for enhancing anti-migration forces[15]. Similarly, flanges can be added to the ends of ureteral SEMS, although their ability to enhance anti-migration forces and the optimal design is unknown. The purpose of this ex vivo study was to evaluate the anti-migration forces of ureteral SEMS with various flange designs.

Department of Interventional Radiology, Guangdong Provincial People's Hospital, Guangdong Academy of Medical Sciences, Southern Medical University, Guangzhou, Guangdong 510080, China. ✉email: fejr@foxmail.com

Methods

Ex vivo model and experimental design

Fresh porcine ureters harvested from domestic pigs weighing 75–100 kg, were obtained from a local abattoir. The ureters were randomly assigned to groups (24 ureters per group), with one type of SEMS placed into the ureters within each group. For each group, 12 ureters were used to evaluate proximal anti-migration forces, while the remaining 12 were used to evaluate distal anti-migration forces. Each SEMS was reused 24 times, once for each ureter in its respective group, due to the high cost of the stents. Before each reuse, a detailed visual inspection of the stent was performed using a digital microscope (TX5300; Seepack, Shenzhen, China) to confirm the absence of any structural damage.

Evaluation of flange designs for SEMS

In the initial study, 240 fresh porcine ureters were used, divided into ten groups to evaluate ten types of SEMS (Type I–X) (Fig. 1a). The SEMS were custom-manufactured by Youan Medical (Beijing, China) according to our specifications. To ensure a fair comparison, all SEMS were fabricated from a single thread of 0.16-mm nitinol wire using the same knitting technique. Each stent measured 5 cm in length and was fully covered with a silicone membrane. Two types lacked flange designs, with diameters of 8 mm (Type I) and 10 mm (Type II), respectively. The remaining eight types (Type III–X) featured various flange designs at the proximal end. For these flanged SEMS, the non-flanged portion measured 8 mm in diameter, while the flanged portion was limited to a length of ≤ 2 cm and a maximum diameter of 10 mm.

Comparison with commercial SEMS

In the subsequent study, 96 fresh porcine ureters were used and divided into four groups to evaluate four types of SEMS (Table 1). The first type was a prototype custom-manufactured by Youan Medical (Beijing, China) according to our specifications (Fig. 1b). It was knitted from a single thread of 0.16-mm nitinol wire and fully covered with a silicone membrane. The proximal end featured a flange design identical to Type X (double-stepped shoulders), which demonstrated the highest distal anti-migration force in the initial study. The non-flanged portion measured 8 mm in diameter, while the 2-cm-long flanged portion had a maximum diameter of 10 mm. The remaining three types of SEMS were commercially available and purchased from distributors: the 7-mm-diameter Urexel (S&G Biotech, Yongin, Korea), the 7-mm-diameter Uventa (Taewoong Medical, Gimpo, Korea), and the 10-mm-diameter Allium (Allium Medical, Caesarea, Israel). These SEMS were also commercially available in other diameters; however, the selected sizes were the most commonly used for their respective types, as reported in the literature, and were therefore chosen for this study[2,3,9]. To ensure a fair comparison, all SEMS were 12 cm in length. Before assessing anti-migration forces, all SEMS were evaluated for their radial force and crush resistance.

SEMS placement procedure

All SEMS were placed using a 10-Fr introducer set (Flexor Check-Flo; Cook Medical, IN, USA). A drawstring was first attached to either the proximal or distal end of the SEMS, depending on whether the proximal or distal anti-migration force was being evaluated. This was achieved by threading the drawstring through each mesh opening at one end of the stent, forming a loop that encompassed its entire circumference (Fig. 1c). As a result, when the drawstring was pulled, the force was distributed more evenly rather than being applied at a single point (Fig. 1d). Each SEMS was then loaded into the introducer sheath through its distal end using a stent crimper (RRC; Blockwise Engineering, AZ, USA). The sheath was subsequently inserted into the porcine ureter from its proximal end. Under direct visualization through the semi-transparent ureter wall, the SEMS was placed in the mid-ureter by using the dilator to maintain the stent's position as the sheath was withdrawn. After allowing a 30-minute period for the SEMS to fully expand within the ureter, the anti-migration force was evaluated.

Anti-migration force evaluation

The anti-migration forces of each SEMS were evaluated using a universal testing machine (KY5000N; Kaiyan Testing Instruments, Shanghai, China) equipped with the manufacturer's original clamps. For proximal anti-migration force evaluation, the distal end of the porcine ureter was secured to the bottom clamp mounted on the stationary crosshead, while a drawstring attached to the proximal end of the SEMS was secured to the upper clamp mounted to the movable crosshead. The movable crosshead was programmed to move at 5 mm per second until the SEMS was completely extracted through the proximal end of the ureter. The maximum force measured during this process was defined as the proximal anti-migration force. For distal anti-migration force evaluation, the proximal end of the porcine ureter was secured to the bottom clamp mounted on the stationary crosshead, while a drawstring attached to the distal end of the SEMS was secured to the upper clamp mounted to the movable crosshead. The movable crosshead was programmed to move at a rate of 5 mm per second until the SEMS was completely extracted through the distal end of the ureter. The maximum force measured during this process was defined as the distal anti-migration force. During testing, ureters were kept moist with saline at room temperature to prevent tissue drying. After the SEMS was extracted from the ureter, the ureter was opened along its longitudinal axis and carefully examined visually to determine whether the stent had caused any tissue injury.

Radial force and crush resistance evaluation

Methods for radial force and crush resistance evaluation are detailed in Supplementary Information.

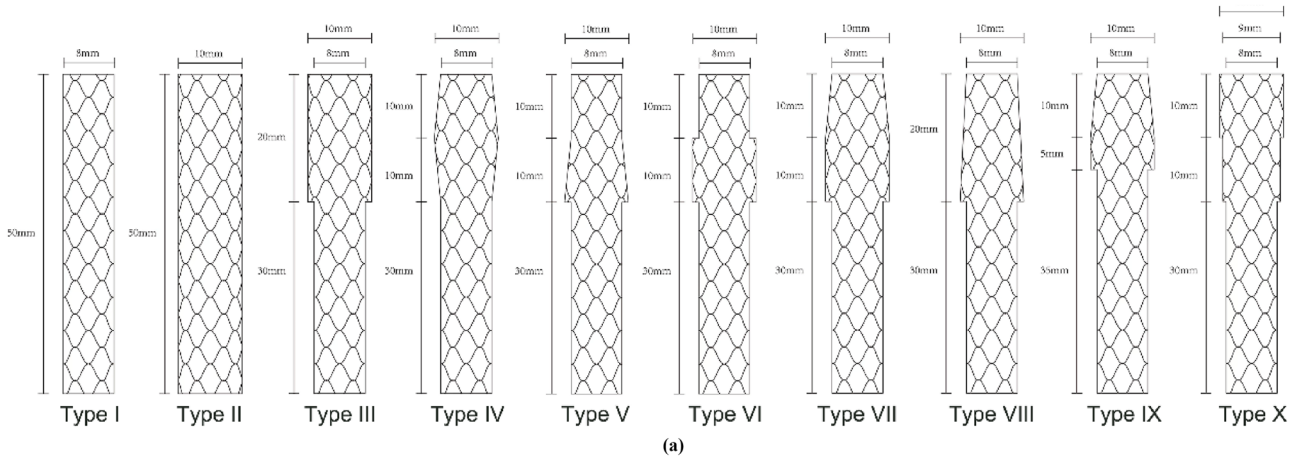

(a)

(b)

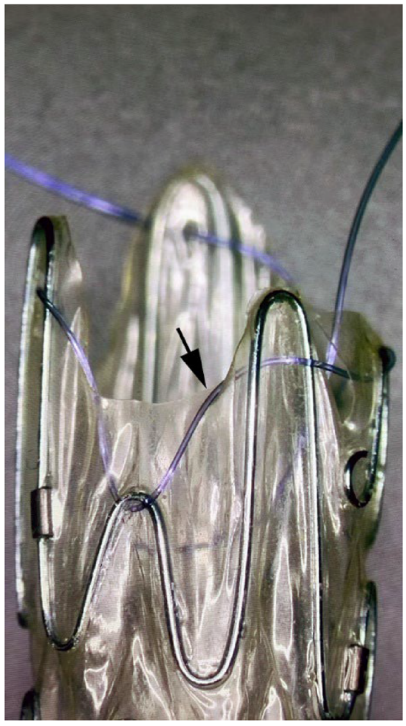

(c)

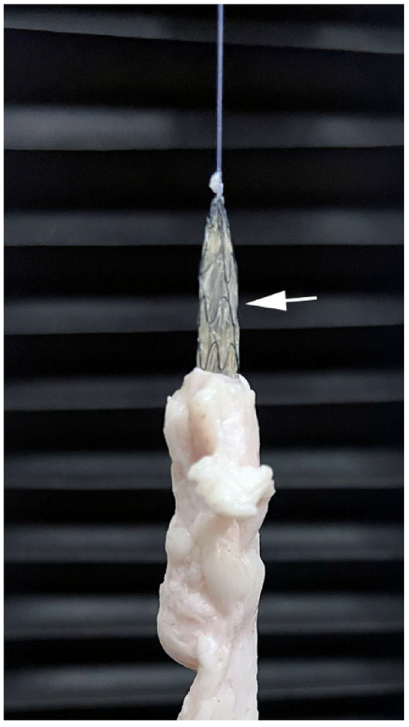

(c)

Fig. 1. (**a**) Schematic representation of the ten types of self-expanding metal stent evaluated in the initial study. **(b)** Photograph showing the four self-expanding metal stent types evaluated in the subsequent study. From left to right: the 8-mm-diameter prototype (Youan Medical, Beijing, China), the 10-mm-diameter Allium (Allium Medical, Caesarea, Israel), the 7-mm-diameter Urexel (S&G Biotech, Yongin, Korea), and the 7-mm-diameter Uventa (Taewoong Medical, Gimpo, Korea). **(c)** Photographs showing the drawstring (arrow) attached to the proximal end of the 10-mm-diameter Allium (Allium Medical, Caesarea, Israel). **(d)** 8-mm-diameter prototype (Youan Medical, Beijing, China) (arrow) being extracted through the proximal end of the porcine ureter during anti-migration testing.

Statistical analysis

Statistical analyses were performed to assess differences in anti-migration forces among SEMS types. One-way ANOVA was used to detect significant differences, with Welch's ANOVA applied when the assumption of equal variances was violated. In the initial study, Dunnett's test was used for post hoc comparisons, as all groups were compared against the 8-mm-diameter non-flanged SEMS. In the subsequent study, Tukey's HSD was applied for pairwise comparisons among all groups, and the Games-Howell test was used when variances were unequal. A P value < 0.05 indicated statistical significance. All statistical analyses were performed with SPSS Statistics v21.0 (IBM, NY, USA).

Name	Manufacture	Type	Mesh	Membrane	Anti-migration features	Diameter*
Prototype	Youan Medical	Fully-covered, knitted, closed-cell	Nitinol	Silicone	Proximal double-step shoulders	8 mm
Urexel	S&G Biotech	Fully-covered, knitted, closed-cell	Nitinol	Silicone	Proximal double layer and flare	7 mm
Uventa	Taewoong Medical	Fully-covered, knitted, closed-cell	Nitinol	PTFE	Full-length double layer	7 mm
Allium	Allium Medical	Fully-covered, knitted, open-cell	Nitinol	PU	None	10 mm

Table 1. Specifications of the four types of SEMS evaluated in the subsequent study.
PTFE = polytetrafluoroethylene; PU = polyurethane. * Indicates the diameter of the non-flanged portion.

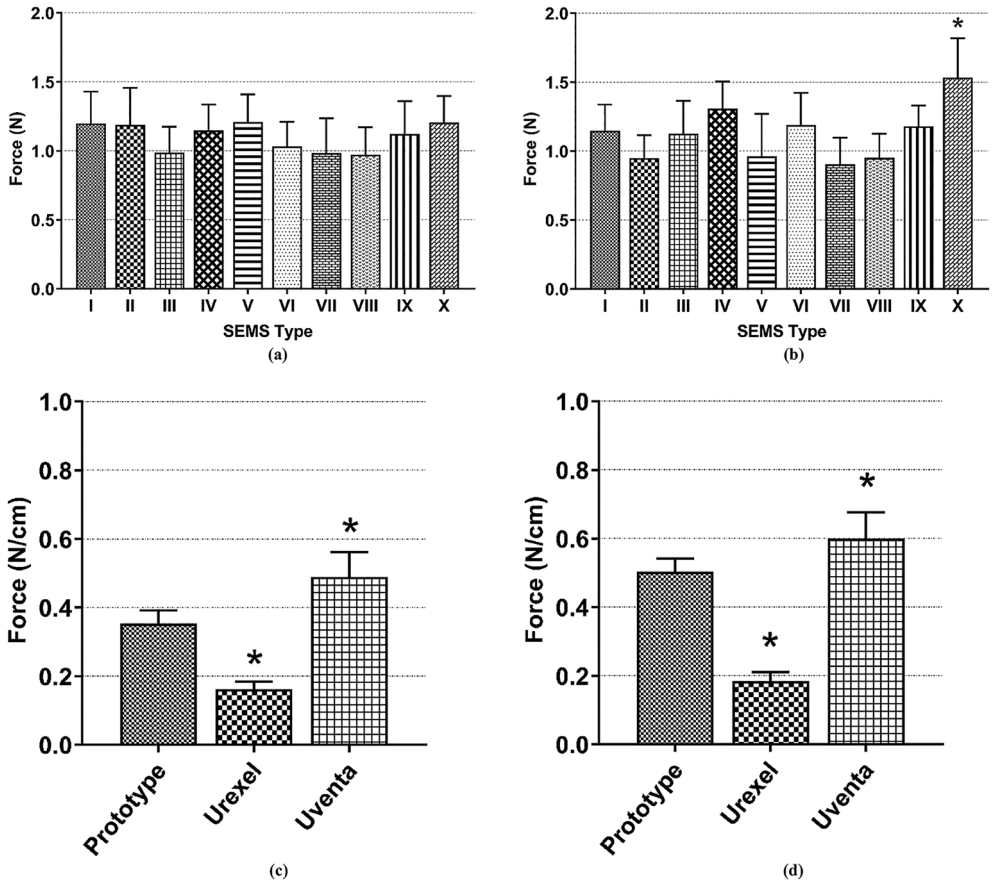

Fig. 2. **(a)** Bar graphs showing the proximal anti-migration force of SEMS evaluated in the initial study. The error bars represent the standard deviation of twelve measurements. * Denotes a statistically significant difference in distal anti-migration force compared with the 8-mm-diameter non-flanged SEMS (Type I). **(b)** Bar graphs showing the distal anti-migration force of SEMS evaluated in the initial study. The error bars represent the standard deviation of twelve measurements. * Denotes a statistically significant difference in distal anti-migration force compared with the 8-mm-diameter non-flanged SEMS (Type I). **(c)** Bar graphs showing the proximal anti-migration force of SEMS evaluated in the subsequent study. The error bars represent the standard deviation of three measurements. * Denotes a statistically significant difference in anti-migration force compared with the prototype. **(d)** Bar graphs showing the distal anti-migration force of SEMS evaluated in the subsequent study. The error bars represent the standard deviation of three measurements. * Denotes a statistically significant difference in anti-migration force compared with the prototype.

Results

Evaluation of flange designs for SEMS

Despite being reused across 24 ureters per group, none of the SEMS exhibited visible structural damage when inspected under the digital microscope. Both proximal and distal anti-migration forces were measured 12 times for each SEMS type, and significant differences were observed among types ($P = 0.025$ and $P < 0.001$, respectively). However, post hoc pairwise comparisons revealed no significant differences in proximal anti-migration force between SEMS types (all $P > 0.05$) (Fig. 2a). For distal anti-migration force, the double-stepped shoulders design (Type X) demonstrated significantly higher values than the 8-mm-diameter non-flanged SEMS (Type I) (1.53 ± 0.29 N vs. 1.15 ± 0.19 N; $P = 0.001$) (Fig. 2b). None of the other flanged SEMS (Types III–IX)

showed a statistically significant difference compared with Type I (all P values > 0.05). Additionally, there was no significant difference between Type I and the 10-mm-diameter non-flanged SEMS (Type II) (1.15 ± 0.19 N vs. 0.95 ± 0.17 N; $P = 1.000$). After SEMS extraction, each ureter was opened longitudinally, and visual examination confirmed the absence of tissue injury (e.g., abrasion, tearing, or perforation) in all samples across the groups.

Comparison with commercial SEMS

Allium unraveled during the initial anti-migration test and was therefore excluded from the analysis. The remaining three SEMS showed no visible structural damage under digital microscopic inspection, despite being reused in 24 ureters per group. Both proximal and distal anti-migration forces were measured 12 times for each SEMS type, and significant differences were observed among types ($P < 0.001$ and $P < 0.001$, respectively) (Fig. 2c and d). For proximal anti-migration force, Uventa showed significantly higher values than the prototype (0.49 ± 0.07 N/cm vs. 0.35 ± 0.04 N/cm; $P < 0.001$) and Urexel (0.49 ± 0.07 N/cm vs. 0.16 ± 0.02 N/cm N/cm; $P < 0.001$), and the prototype showed significantly higher values than Urexel (0.35 ± 0.04 N/cm vs. 0.16 ± 0.02 N/cm; $P < 0.001$). Similarly, for distal anti-migration force, Uventa showed significantly higher values than the prototype (0.60 ± 0.08 N/cm vs. 0.50 ± 0.04 N/cm; $P = 0.001$) and Urexel (0.50 ± 0.04 N/cm vs. 0.18 ± 0.03 N/cm; $P < 0.001$), and the prototype showed significantly higher values than Urexel (0.50 ± 0.04 N/cm vs. 0.18 ± 0.03 N/cm; $P < 0.001$). Following SEMS extraction, the ureters were longitudinally opened, and visual inspection confirmed no tissue injury (e.g., abrasion, tearing, or perforation) in any of the samples across the groups.

Radial force and crush resistance

The radial resistive force (RRF) and chronic outward force (COF) were each measured three times for each SEMS type. Uventa demonstrated the highest RRF and COF (1.75 ± 0.04 N/mm and 1.68 ± 0.04 N/mm, respectively), followed by the prototype (1.17 ± 0.04 N/mm and 1.17 ± 0.03 N/mm, respectively), Allium (0.97 ± 0.01 N/mm and 0.87 ± 0.01 N/mm, respectively), and Urexel (0.75 ± 0.01 N/mm and 0.73 ± 0.01 N/mm, respectively) (Supplementary Fig. 1). For crush resistance (measured three times for each SEMS type), Uventa (0.16 ± 0.01 N/mm) again showed the highest values, followed by Urexel (0.12 ± 0.01 N/mm), the prototype (0.08 ± 0.01 N/mm), and Allium (0.06 ± 0.01 N/mm) (Supplementary Fig. 2).

Discussion

Stent migration remains a major limitation of ureteral SEMS, often occurring shortly after placement, leading to early re-obstruction and typically requiring removal via minimally invasive techniques or open surgery[9–11]. In the esophagus, SEMS with flanges at both ends have become standard; the proximal flange mitigates distal migration, while the distal flange mitigates proximal migration[15]. The small caliber of biliary and ureteral SEMS has historically posed challenges to the integration of flange structures. However, recent advances in SEMS technology have enabled the incorporation of complex flanges into small-caliber SEMS, and several biliary SEMS with such designs are now commercially available[16–18]. Nonetheless, whether the anti-migration forces of ureteral SEMS can be enhanced through the incorporation of flanges remains uncertain.

In this study, the anti-migration forces of eight flanged SEMS designs were compared with an 8-mm-diameter non-flanged SEMS. Only the double-stepped shoulders design (Type X) showed a statistically significant increase in distal anti-migration force. None of the other flange types differed significantly from the non-flanged control. This includes the barrel design (Type IV), which previously demonstrated significantly higher distal anti-migration force than the dumbbell design (Type III) and the flare design (not evaluated in our study) in a esophageal SEMS bench-top study[19]. This discrepancy likely reflects the differing capacities of the esophagus and ureter to accommodate larger-diameter flanges. Whereas the esophageal lumen can accommodate flanges several millimeters larger in diameter than the stent body, the ureter's narrower lumen permits only a minimal increase. Therefore, ureteral SEMS require flange designs that function optimally within the limited diameter of the ureter. A 10-mm-diameter non-flanged SEMS was also evaluated in this study to determine whether oversizing the stent could increase anti-migration forces. However, it did not exhibit higher anti-migration forces than the 8-mm-diameter non-flanged SEMS. This finding suggests that oversizing alone may not reduce migration risk.

Besides flanges, other anti-migration features have been developed for non-vascular SEMS. Barbs were previously used in esophageal, tracheal, and urethral SEMS but have fallen out of favor due to their tendency to cause pain[20–22]. Double-layer designs involve the addition of a second bare stent layer over the covered layer to enhance anti-migration force [2; 9]. Such designs have been applied to ureteral SEMS; however, Uventa, which features a full-length double-layer design, has raised concerns due to major complications, including fistula formation, ureteral perforation, and uncontrollable bleeding[9]. In addition, tissue or tumor ingrowth into the bare outer layer may occur, potentially rendering the stent impossible to remove[9]. By contrast, Urexel, which incorporates a double-layer design only at the proximal end, has not been associated with these complications[2]. However, as demonstrated in the present study, Urexel's anti-migration forces were significantly lower than those of Uventa.

In the literature, reported stent migration rates range from 2 to 23% for Urexel[2,11], 3–22% for Uventa[9,23], and 14–24% for Allium[10,24]. Notably, Allium lacks anti-migration features, which likely accounts for its higher migration rates. To evaluate whether a SEMS with double-stepped shoulders provides anti-migration force comparable to that of commercial SEMS, we constructed a prototype featuring this flange design at the proximal end and compared it against Urexel, Uventa, and Allium. The results showed that the prototype's anti-migration forces were significantly higher than those of Urexel but lower than those of Uventa. This is an encouraging finding given the prototype's lack of a double-layer design.

This study has several limitations. First, it was conducted using an ex vivo static model that cannot replicate the dynamic physiological processes of the ureter (e.g., peristalsis and urine flow). Both primarily act in the

distal direction and generate repetitive mechanical forces that may promote stent migration. Over time, tissue hyperplasia and encrustation may increase anchoring strength and thereby reduce migration. Second, the porcine ureters were structurally normal and lacked pathological features such as luminal narrowing or hydronephrotic dilation. Third, each SEMS was reused multiple times because of the high cost of the stent, and this reuse may have affected the stent's mechanical properties. Nevertheless, reuse was deemed acceptable, as every stent was carefully inspected under a digital microscope before testing to confirm the absence of deformation, wire breakage, or membrane damage. Although mechanical properties were not reassessed quantitatively, the anti-migration force values remained within a consistent range across repeated tests, suggesting that any effect of reuse was minimal. Finally, there is currently no evidence to determine how anti-migration forces measured under experimental conditions relate to clinical migration risk. Nevertheless, these data remain valuable, as they provide a quantitative benchmark for comparing stent designs and identifying which configurations are more likely to migrate.

In conclusion, in an ex vivo porcine ureter model, only the double-stepped shoulders significantly improved distal anti-migration force among eight flange designs. When compared with commercial SEMS, the prototype featuring the double-stepped shoulders demonstrated anti-migration forces significantly higher than those of Urexel but lower than those of Uventa. However, as this was an ex vivo study, the findings remain preliminary and require confirmation in in vivo or clinical settings.

Data availability

The data that support the findings of this study are available from the corresponding author upon reasonable request.

Received: 12 September 2025; Accepted: 4 November 2025
Published online: 26 November 2025

References

1. Cao, C. et al. Temporary covered metallic ureteral stent placement for ureteral strictures following kidney transplantation: experience in 8 patients. *J. Vasc Interv Radiol.* **31**, 1795–1800. https://doi.org/10.1016/j.jvir.2020.04.004 (2020).
2. Tsauo, J., Shin, J. H., Kim, G. H. & Chu, H. H. A Silicone-Covered Self-Expanding metal stent with Anti-migration features for treating malignant ureteral obstruction. *Cardiovasc. Intervent Radiol.* **45**, 1503–1511. https://doi.org/10.1007/s00270-022-03174-3 (2022).
3. Gao, X. et al. Metal ureteral stents for ureteral stricture: 2 years of experience with 246 cases. *Int. J. Surg.* **110**, 66–71. https://doi.org/10.1097/js9.0000000000000841 (2024).
4. Chung, H. H. et al. Multicenter experience of the newly designed covered metallic ureteral stent for malignant ureteral occlusion: comparison with double J stent insertion. *Cardiovasc. Intervent Radiol.* **37**, 463–470. https://doi.org/10.1007/s00270-013-0675-2 (2014).
5. Kim, J. W. et al. A prospective randomized comparison of a covered metallic ureteral stent and a Double-J stent for malignant ureteral obstruction. *Korean J. Radiol.* **19**, 606–612. https://doi.org/10.3348/kjr.2018.19.4.606 (2018).
6. Kim, E. T. et al. Comparison of a covered metallic ureteral stent and a double-J stent for malignant ureteral obstruction in advanced gastric cancer. *Clin. Radiol.* **76**, 519–525. https://doi.org/10.1016/j.crad.2021.02.016 (2021).
7. Barbalias, G. A. et al. Externally coated ureteral metallic stents: an unfavorable clinical experience. *Eur. Urol.* **42**, 276–280. https://doi.org/10.1016/s0302-2838(02)00281-6 (2002).
8. Liatsikos, E. N. et al. Ureteral metal stents: 10-year experience with malignant ureteral obstruction treatment. *J. Urol.* **182**, 2613–2617. https://doi.org/10.1016/j.juro.2009.08.040 (2009).
9. Kim, M., Hong, B. & Park, H. K. Long-Term outcomes of Double-Layered polytetrafluoroethylene Membrane-Covered Self-Expandable segmental metallic stents (Uventa) in patients with chronic ureteral obstructions: is it really safe? *J. Endourol.* **30**, 1339–1346. https://doi.org/10.1089/end.2016.0462 (2016).
10. Gao, X. et al. Self-expanding metal ureteral stent for ureteral stricture: experience of a large-scale prospective study from a high-volume center - Cross-sectional study. *Int. J. Surg.* **95**, 106161. https://doi.org/10.1016/j.ijsu.2021.106161 (2021).
11. Lee, C. U., Choo, S. H., Chung, J. H. & Han, D. H. Initial experience of a novel ureteral silicon-covered metallic mesh stent in malignant ureteric obstruction: a single-center retrospective study. *BMC Urol.* **24**, 268. https://doi.org/10.1186/s12894-024-01653-y (2024).
12. Liatsikos, E. N. et al. Coated v noncoated ureteral metal stents: an experimental model. *J. Endourol.* **15**, 747–751. https://doi.org/10.1089/08927790152596361 (2001).
13. Pollak, J. S., Rosenblatt, M. M., Egglin, T. K., Dickey, K. W. & Glickman, M. Treatment of ureteral obstructions with the Wallstent endoprosthesis: preliminary results. *J. Vasc Interv Radiol.* **6**, 417–425. https://doi.org/10.1016/s1051-0443(95)72833-0 (1995).
14. Lugmayr, H. F. & Pauer, W. Wallstents for the treatment of extrinsic malignant ureteral obstruction: midterm results. *Radiology* **198**, 105–108. https://doi.org/10.1148/radiology.198.1.8539359 (1996).
15. Kim, K. Y., Tsauo, J., Song, H. Y., Kim, P. H. & Park, J. H. Self-Expandable metallic stent placement for the palliation of esophageal cancer. *J. Korean Med. Sci.* **32**, 1062–1071. https://doi.org/10.3346/jkms.2017.32.7.1062 (2017).
16. Bordaçahar, B. et al. Clinical efficacy of anti-migration features in fully covered metallic stents for anastomotic biliary strictures after liver transplantation: comparison of conventional and anti-migration stents. *Gastrointest. Endosc.* **88**, 655–664. https://doi.org/10.1016/j.gie.2018.06.035 (2018).
17. Miyazawa, M. et al. Efficacy of a novel self-expandable metal stent with dumbbell-shaped flare ends for distal biliary obstruction due to unresectable pancreatic cancer. *Sci. Rep.* **12**, 21100. https://doi.org/10.1038/s41598-022-25186-2 (2022).
18. Tsauo, J. et al. Characteristics of four commonly used self-expanding biliary stents: an in vitro study. *Eur. Radiol. Exp.* **8**, 24. https://doi.org/10.1186/s41747-024-00425-5 (2024).
19. Maetani, I., Shigoka, H., Omuta, S., Gon, K. & Saito, M. What is the preferred shape for an esophageal stent flange? *Dig. Endosc.* **24**, 401–406. https://doi.org/10.1111/j.1443-1661.2012.01299.x (2012).
20. Song, H. Y., Choi, K. C., Cho, B. H., Ahn, D. S. & Kim, K. S. Esophagogastric neoplasms: palliation with a modified Gianturco stent. *Radiology* **180**, 349–354. https://doi.org/10.1148/radiology.180.2.1712500 (1991).
21. Kim, Y. H., Shin, J. H., Song, H. Y. & Kim, J. H. Tracheal stricture and fistula: management with a barbed silicone-covered retrievable expandable nitinol stent. *AJR Am. J. Roentgenol.* **194**, W232–237. https://doi.org/10.2214/ajr.09.3025 (2010).
22. Choi, S. Y. et al. Efficacy and tolerability of metallic stent in patients with malignant prostatic obstruction secondary to prostatic cancer. *Low Urin Tract. Symptoms*. **13**, 329–334. https://doi.org/10.1111/luts.12367 (2021).

23. Chung, K. J. et al. Efficacy and safety of a novel, double-layered, coated, self-expandable metallic mesh stent (Uventa™) in malignant ureteral obstructions. *J. Endourol.* **27**, 930–935. https://doi.org/10.1089/end.2013.0087 (2013).
24. Moskovitz, B., Halachmi, S. & Nativ, O. A new self-expanding, large-caliber ureteral stent: results of a multicenter experience. *J. Endourol.* **26**, 1523–1527. https://doi.org/10.1089/end.2012.0279 (2012).

Author contributions

J.T., Z.M., Q.W., Q.G., Q.M., Z.C., and J.Z. contributed to the study conception and design. J.T., Z.M., and Q.W. performed the material preparation, data collection, and analysis.J.T. wrote the first draft of the manuscript.J.T., Z.M., Q.W., Q.G., Q.M., Z.C., and J.Z. commented on previous versions of the manuscript.J.T., Z.M., Q.W., Q.G., Q.M., Z.C., and J.Z. read and approved the final manuscript.

Funding

The authors did not receive support from any organization for the submitted work.

Declarations

Competing interests

The authors declare no competing interests.

Ethical approval

As the tissue samples used in this study were byproducts of animals slaughtered for commercial purposes and not specifically harvested for research, approval from the Institutional Animal Research Committee was not required.

Additional information

Supplementary Information The online version contains supplementary material available at https://doi.org/10.1038/s41598-025-27443-6.

Correspondence and requests for materials should be addressed to J.Z.